JOURNAL OF APPLIED POLYMER SCIENCE VOL. 18, PP. 567–588 (1974)

Reverse Osmosis Separation of Single and Mixed Alcohols in Aqueous Solutions Using Porous Cellulose Acetate Membranes

TAKESHI MATSUURA, M. E. BEDNAS, and S. SOURIRAJAN,
Division of Chemistry, National Research Council of Canada, Ottawa, Canada

Synopsis

Reverse osmosis transport for alcohol–water systems in the Taft number (σ^*) region of 0 to -0.3 is explored in detail. The numerical value of the polar functional constant for alcohols is 15.5 for the above σ^* region in the operating pressure range of 50 to 500 psig for the cellulose acetate membrane material used. An analysis of the combined effect of operating pressure and mass transfer coefficient on the high-pressure side of the membrane shows that, under certain conditions, solute separation could pass through a maximum with increase in operating pressure. A general expression for solute separation is derived as a function of pore structure on membrane surface, polarity of solute, and operating conditions of the experiment. Alcohols behave independently in mixed solute systems. A method is described and illustrated for predicting alcohol separation in alcohol–sucrose–water feed solutions from data on single solute systems.

INTRODUCTION

The physicochemical criteria for the reverse osmosis separation of alcohols in aqueous solutions using the Loeb-Sourirajan-type porous cellulose acetate membranes have been discussed.[1–5] It has been shown[5] that solute separation data can be correlated with Taft number (σ^*) for the substituent group in the alcohol molecule and, in small ranges of σ^*, the solute transport parameter ($D_{AM}/K\delta$) for the alcohol[6] and the corresponding Taft number are related by the expression

$$(D_{AM}/K\delta) = C^* \exp(\rho^*\sigma^*) \quad (1)$$

where ρ^* is a polar functional constant for alcohol and C^* is a proportionality constant depending on the porous structure of the membrane. The value of ρ^* is different for different ranges of σ^*, but it is independent of the porous structure of the membrane. Consequently, the numerical value of ρ^* is an important operational parameter in reverse osmosis transport. Combined with the general Kimura-Sourirajan analysis,[6] the use of eq. (1) to estimate $D_{AM}/K\delta$ and predict the separation of different alcohols for a given membrane from a single set of experimental data for a reference solution system has been illustrated.[5] All the previous work has been with single solute systems.

An extension of the above work[5] is reported in this paper. In this work, the σ^* region of 0 to -0.3 is explored in detail. The numerical value of ρ^* for alcohols is more firmly established for the operating pressure range of 50 to 500 psig. The procedure for predicting membrane performance is improved. Reverse osmosis data were obtained for a number of mixed solute systems involving two to five alcohols. The effect of mixed solutes on membrane performance is ascertained. The reverse osmosis separation of an alcohol present in low concentrations in aqueous sucrose feed solutions was also investigated; a method is presented for predicting alcohol separation from such mixed solute systems. This latter investigation is of potential practical interest in predicting membrane performance during concentration of fruit juices by reverse osmosis.

EXPERIMENTAL

Reverse Osmosis Experiments

Eight monohydric alcohols listed in Table I (along with some of their physicochemical data pertinent to this work) were used in this work in single and mixed solute systems. The apparatus and experimental procedure used were the same as those reported earlier.[3,5] Batch 316-type cellulose acetate membranes[7] were used in the operating pressure range of 50 to 500 psig. The specifications[6] of the membranes used are given in Table II in terms of pure water permeability constant A (g mole H_2O/cm^2 sec atm) and solute transport parameter $D_{AM}/K\delta$ for sodium chloride (cm/sec) at 250 psig. Table II also includes solute separation and product rate data for the membranes in the operating pressure range of 50 to 500 psig using 1500 ppm NaCl–H_2O feed solutions at the feed flow conditions used in this work; the latter corresponded to a mass transfer coefficient k of 22×10^{-4} cm/sec on the high-pressure side of the membrane for the above NaCl–H_2O feed solution.

The alcohol concentrations in the feed solutions used were in the range of 0.001 to 0.01 g-mole/l.; in most cases, the alcohol concentration in the feed

TABLE I
Data for the Alcohol-Solutes Studied

Solute no.	Solute: Name	Solute: Formula R in ROH	Solute: Molecular weight	σ^*	$D_{AB} \times 10^5$, cm^2/sec	$k \times 10^4$, cm/sec
1	*t*-Butyl alcohol	*t*-C_4H_9	74.1	−0.300	1.043	16.3
3	*s*-Butyl alcohol	*s*-C_4H_9	74.1	−0.210	1.043	16.3
4	Isopropyl alcohol	i-C_3H_7	60.1	−0.190	1.206	18.0
6	*n*-Butyl alcohol	*n*-C_4H_9	74.1	−0.130	1.043	16.3
7	Isobutyl alcohol	i-C_4H_9	74.1	−0.200	1.043	16.3
8	*n*-Propyl alcohol	*n*-C_3H_7	60.1	−0.115	1.206	18.0
9	Ethyl alcohol	C_2H_5	46.1	−0.100	1.460	20.4
10	Methyl alcohol	CH_3	32.0	0	1.935	24.7

TABLE II
Specification of Membranes and Some Performance Data

	Films				
	1	2	3	4	5
	250 psig				
Pure water permeability constant A, $\left(\frac{\text{g-mole } H_2O}{\text{cm}^2\cdot\text{sec}\cdot\text{atm}}\right) \times 10^6$	1.614	2.614	3.778	2.088	3.620
Solute transport parameter $(D_{AM}/K\delta)_{NaCl}$, (cm/sec) $\times 10^5$	2.101	5.518	16.39	3.82	19.82
Solute separation, %	95.0	90.7	83.3	93.5	77.6
Product rate, g/hr[a]	21.4	34.2	49.8	27.4	47.6
	50 psig				
Solute separation, %	80.4	71.2	57.1	78.4	50.7
Product rate, g/hr[a]	3.8	6.5	10.0	5.0	9.8
	375 psig				
Solute separation, %	95.6	92.9	86.4	94.6	80.4
Product rate, g/hr[a]	33.4	51.5	72.5	42.4	69.2
	500 psig				
Solute separation, %	96.9	94.1	89.0	95.7	83.5
Product rate, g/hr[a]	44.6	68.3	95.2	57.0	90.4

[a] Area of film surface = 13.2 cm².

solution was ~100 ppm. In the mixed solute systems also, the concentration of each alcohol was kept in the above range. In the *t*-butyl alcohol–sucrose–water system, the alcohol molality was fixed as 0.002, and the sucrose molality was changed from 0.115 to 0.585. The osmotic pressure of the feed solution with respect to alcohol was practically negligible in all cases.

All experiments were of the short-run type, and they were carried out at the laboratory temperature (23–25°C). The reported product rates are those corrected to 25°C using the relative viscosity and density data for pure water. In all experiments, the terms "product" and "product rate" refer to membrane-permeated solutions. For the single and mixed alcohol–water systems, the per cent solute separation f with respect to each alcohol was obtained from the relation

$$f = \left(\frac{\text{solute ppm in feed} - \text{solute ppm in product}}{\text{solute ppm in feed}}\right) \times 100. \quad (2)$$

For the *t*-butyl alcohol–sucrose–water systems, the value of f for each solute was obtained from the relation

$$f = \left(\frac{\text{solute molality in feed} - \text{solute molality in product}}{\text{solute molality in feed}}\right) \times 100. \quad (3)$$

In each experiment, the pure water permeation rate (PWP) and the product rate (PR), in grams per hour per given area of film surface (13.2 cm² in all

cases in this work), and the solute separation were determined at the specific operating conditions. The solute numbers given in all figures in this paper are the same as those given in Table I.

Analysis

Single and Mixed Alcohol–Water Solutions. A Perkin Elmer Model 154 gas chromatograph was used to determine alcohol concentrations. The chromatographic column used was a 15-ft-long, $^3/_{16}$ in. in diameter stainless steel tubing packed with 10% diglycerol on 60–80 mesh Neutraport. Helium flow rate through the column was 36 ml/min, and the entire effluent from the column passed into a hydrogen flame ionization detector. The column was operated at 75°C. A sample size of 2 microliters was used for each analysis. For the analysis of *t*-butyl alcohol, isopropyl alcohol, *n*-propyl alcohol, ethyl alcohol, and methyl alcohol in reverse osmosis experiments at 375 psig, 75 ppm methyl ethyl ketone was used as the internal standard; external standards were used in all other analyses.

For the analysis of methanol, the carrier gas was passed through a conditioning column (9 ft × 0.25 in. diameter of 45% water on 30–60 mesh firebrick at 0°C) before the sample injector and analyzing column. This arrangement gave sharper and reproducible methanol peaks which were otherwise unsatisfactory.

***t*-Butyl Alcohol–Sucrose–Water Solutions.** A Tracor Model 160 gas chromatograph was used for the analysis of *t*-butyl alcohol. The chromatographic column used was a 6-ft-long, 0.25 in. in diameter stainless steel tubing packed with 20–30 mesh ascarite for the initial 4.5 in., and with 5% OVI on 80–100 mesh Chromosorb W(HP) for the remaining length. Since the nonvolatile solute remained in the column without being eluted by the carrier gas, the column had to be changed frequently. Helium flow through the column was 60 ml/min, and the entire effluent from the column passed into a hydrogen flame ionization detector. The column was operated at 80°C.

A Beckman total carbon analyzer Model 915 was used to determine total carbon content in the sample. The analytical procedure was the same as that used before.[3,5] A sample size of 20 microliters was used for each analysis. The carbon content corresponding to sucrose in the sample was obtained by the difference between total carbon content and the carbon equivalent of *t*-butyl alcohol determined by gas-chromatographic analysis.

Accuracy. The accuracy of gas-chromatographic analysis was ±2% in all cases. The accuracy of carbon analyzer was ±1 ppm in terms of carbon content.

RESULTS AND DISCUSSION

Single Solute Systems

Taft Number Versus Membrane Performance. Figure 1 gives the correlation of Taft number corresponding to each alcohol versus solute separa-

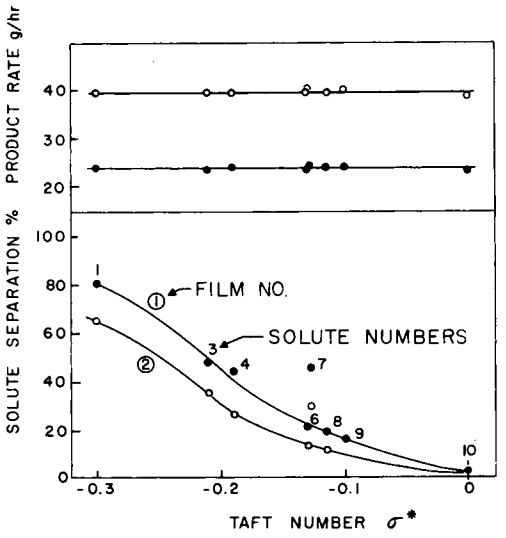

Fig. 1. Effect of Taft number of alcohols on solute separation and product rate: film type, cellulose acetate (Batch 316); operating pressure, 250 psig; feed concentration, 0.0159 g-mole/l. for methanol, 0.0012 ~ 0.0025 g-mole/l. for other alcohols; feed flow rate, 400 cc/min; membrane area, 13.2 cm²; solute numbers and calculated k values, same as in Table I.

tion and product rate for films 1 and 2. The feed concentration, operating pressure, and the feed flow rate used were the same in all cases. For each film, the product rate remained essentially constant for all the systems studied. These data show that the porous structure of the membrane surface was not affected by the alcohols used. The data on solute separation confirm the observation made earlier that, for each film, there exists a unique correlation between Taft number (σ^*) and solute separation. The data for the separation of isobutyl alcohol (solute 7), however, do not fit the general σ^*-versus-solute separation correlation applicable for all the other alcohols studied. The value of σ^* given by Taft for i-C_4H_9 is -0.125; the reverse osmosis separation of isobutyl alcohol is much higher than that predicted by the above correlation. Similar results have been reported earlier.[3,5] Since it has now been established[5] that the σ^*-versus-solute separation correlation for alcohols is precise and quantitative, the above correlation can also serve as a basis for assigning appropriate σ^* values for new or exceptional solutes. The σ^* values so assigned may be expected to be valid for predicting solute transport in reverse osmosis. The success of this technique has already been illustrated with respect to the reverse osmosis separation of cyclohexanol and cyclohexanediols.[5]

In order to assign an appropriate value of σ^* for i-C_4H_9 for use in reverse osmosis, the σ^*-versus-solute separation correlation for alcohols corresponding to the limiting condition of $k = \infty$ (where k is the mass transfer coefficient on the high-pressure side of the membrane) must be established first so that the above correlation is independent of the effect of concentration

polarization on solute separation. The value of fraction solute separation at $k = \infty$ (designated as f_∞) may be calculated from the experimental solute separation (f) and product rate (PR) data as follows.

First, calculate k for the experimental conditions used from the relation

$$k = k_{\text{ref}} \left[\frac{D_{AB}}{(D_{AB})_{\text{ref}}} \right]^{2/3} \tag{4}$$

where k_{ref} = mass transfer coefficient on the high-pressure side of the membrane for the reference solution system sodium chloride–water, and $(D_{AB})_{\text{ref}}$ and D_{AB} refer to diffusivity of sodium chloride and alcohol, respectively, in water. The value of D_{AB} may be calculated as before from the empirical equation of Wilke and Chang.[5,9] The above values of k are included in Table I.

Next, using the above value of k and experimental f and PR data, calculate the solute transport parameter ($D_{AM}/K\delta$) for the alcohol from the relation

$$\left(\frac{D_{AM}}{K\delta}\right) = \frac{(PR)}{3600\ S\ d} \frac{(1-f)}{f} \left[\frac{1}{\exp\left\{ \frac{(PR)}{3600\ S\ k\ d} \right\}} \right] \tag{5}$$

where S = effective membrane area (cm^2) and d = solution density (g/cm^3).

Finally, using the above value of $D_{AM}/K\delta$, calculate f_∞ from the relation

$$f_\infty = \left[1 + \frac{(D_{AM}/K\delta)\ 3600\ S\ d}{(PR)} \right]^{-1} \tag{6}$$

Equation (5) has been derived.[5] Equation (6) follows from eq. (5) when $k = \infty$. Equation (4) needs an explanation.

In the previous paper,[5] k was calculated from eq. (4) with unity as the exponent on the right-hand side of the equation. This was based on the assumption that with respect to a given apparatus, for the same conditions of feed concentration and feed flow rate, the thickness of the concentrated boundary layer on the high-pressure side of the membrane is constant for different solutions. In view of the excellent agreement illustrated in the paper[5] between the experimental and calculated solute separation data based on the values of k so obtained, the above assumption seemed acceptable at least for the experimental conditions tested. However, the generalized correlation for mass transfer coefficients discussed extensively in the literature[6] offers a firm experimental basis for the calculation of k. According to the above correlation, at a given Reynold's number (N_{Re}), the quantity $N_{\text{Sh}}/(N_{\text{Sc}})^{1/3}$ is a constant, where N_{Sh} and N_{Sc} represent Sherwood number and Schmidt number, respectively. Defining

$$N_{\text{Re}} = \frac{Q}{h\nu} \tag{7}$$

$$N_{\text{Sh}} = \frac{kd}{D_{AB}} \tag{8}$$

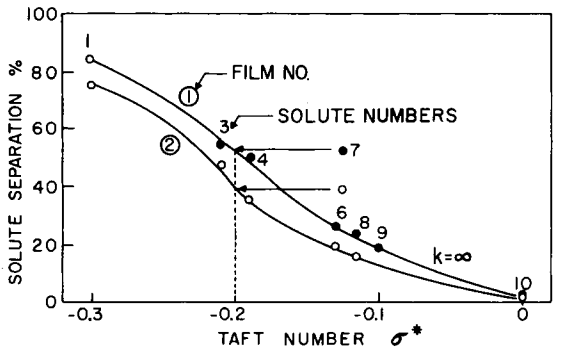

Figure 2. Solute separation of alcohols at $k = \infty$. Other experimental conditions same as for Fig. 1.

and

$$N_{Sc} = \frac{\nu}{D_{AB}} \tag{9}$$

where Q = feed flow rate, h = depth of cell, d = diameter of membrane surface, and ν = kinematic viscosity of solution, it may be seen that with a given apparatus (i.e., constant h and d) and feed solutions of constant viscosity (ν is essentially the same as that of water in the present work), at a given feed flow rate, the quantity $k/(D_{AB})^{2/3}$ is constant for all solutes, which is the basis of eq. (4).

The correlations of σ^* versus f_∞ obtained from eq. (6) for films 1 and 2 are given in Figure 2, which shows that the value of σ^* corresponding to the separation data for isobutyl alcohol is -0.20, and the latter value is independent of the porous structure of the membrane considered. On the basis of Figure 2, a value of -0.20 was assigned as the σ^* for i-C_4H_9 for purposes of correlation of reverse osmosis data, and the above value is used in the rest of this paper.

Polar Functional Constant ρ^* for Alcohols. Numerical values of ρ^* are needed for use in eq. (1) to determine the applicable value of the proportionality constant C^* for a given membrane (which value depends on the porous structure of the membrane) and the values of $D_{AM}/K\delta$ for different alcohols from the data for a reference alcohol–water system. In the previous work,[5] the value of ρ^* was obtained by plotting σ^* versus experimental $D_{AM}/K\delta$ data for different alcohols in a semilog plot and determining the slope of the best straight line drawn arbitrarily to represent the experimental points. The arbitrariness in drawing the best straight line in the above plot can be avoided by using the least-squares technique to treat the experimental data to obtain ρ^* and C^*. This method was followed in this work to obtain the values of ρ^* and C^* for films 1, 2, and 3 in the σ^* range of 0 to -0.3 at the operating pressures of 250, 375, and 500 psig. The results obtained are given in Table III.

TABLE III
Values of ρ^* and C^* for Films 1, 2, and 3

Films	1	2	3	Av. ρ^* for three membranes
Operating pressure, psig		ρ^* values		
250	15.9	13.0	15.2	14.7
375	16.6	16.8	15.5	16.3
500	16.1	13.8	16.5	15.5
Av. ρ^* for three pressures	16.2	14.5	15.7	15.5
Operating pressure, psig		ln C^* values		
250	−4.55	−4.04	−3.00	
375	−4.24	−3.12	−3.04	
500	−4.58	−3.93	−2.93	
Av. ln C^* for three pressures	−4.46	−3.70	−2.99	

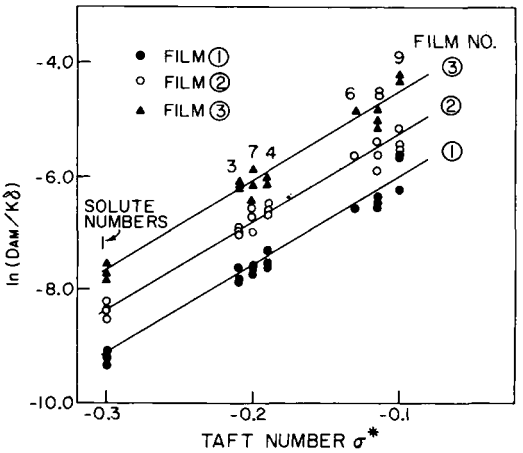

Fig. 3. Effect of Taft number on solute transport parameter for alcohols: film type, cellulose acetate (Batch 316); operating pressures, 250, 375, and 500 psig; solute numbers, same as in Table I.

On the basis that the value of ρ^* is independent of the porous structure on the membrane surface, the average values of ρ^* for films 1, 2, and 3 were found to be 14.7, 16.3, and 15.5 at 250, 375, and 500 psig, respectively. The variation among the above values of ρ^* is no more than that obtained for the three films at the same pressure. Consequently, it seemed reasonable to conclude that in the operating pressure range 250 to 500 psig, the values of ρ^* did not change significantly, and hence a constant value of $\rho^* = 15.5$ (average of all the ρ^* values obtained) could be used for the type of films used in the operating pressure range of 250 to 500 psig for all alcohols in the σ^* range of 0 to −0.3.

There was no significant difference in the values of C^* in the operating pressure range of 250 to 500 psig for each film. This result indicates that

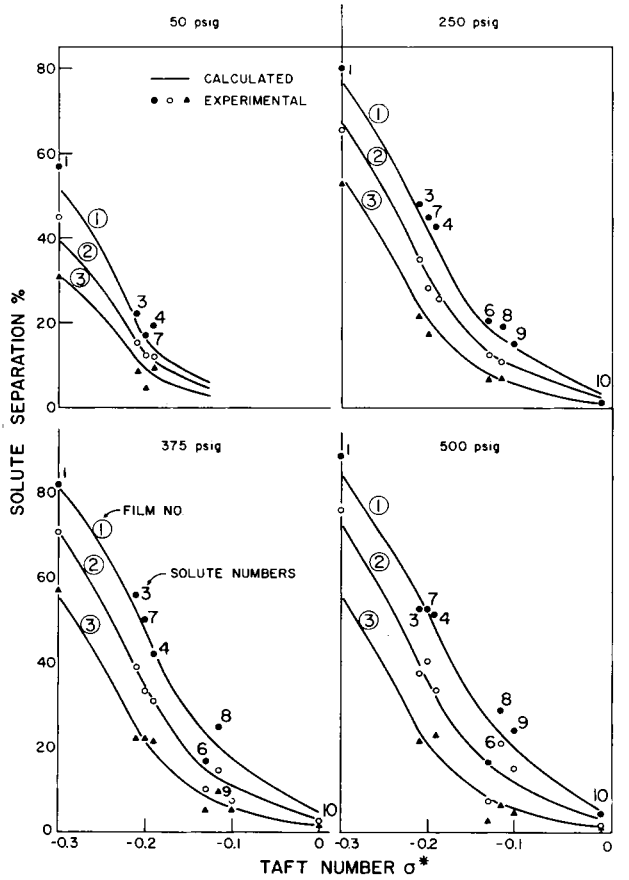

Fig. 4. Effect of Taft number on solute separation for alcohols for films 1, 2, and 3: (——) predicted (●) (○) (▲) experimental; film type, cellulose acetate (Batch 316); operating pressures, 50, 250, 375, and 500 psig; feed flow rate, 400 cc/min; solute numbers, same as in Table I.

there was no change in the porous structure of the membrane surface in the operating pressure range studied. Consequently, an average value of C^* for each film was used in subsequent calculations.

Figure 3 shows the plots of $\ln(D_{AM}/K\delta)$ (obtained experimentally) versus σ^* for films 1, 2, and 3 at the operating pressures of 250, 375, and 500 psig, along with the straight-line correlations representing eq. (1) with $\rho^* = 15.5$ for all films, and $C^* = -4.46$, -3.70, and -2.99 for films 1, 2, and 3, respectively (Table III) applicable for the operating pressure range of 250 to 500 psig. The plots show that the straight-line correlations represent the experimental data reasonably well; this was verified by two independent tests.

In the first test, taking $\rho^* = 15.5$ and $\ln C^* = -4.46$, -3.70, and -2.99 for films 1, 2, and 3, respectively, for all pressures, and assuming that

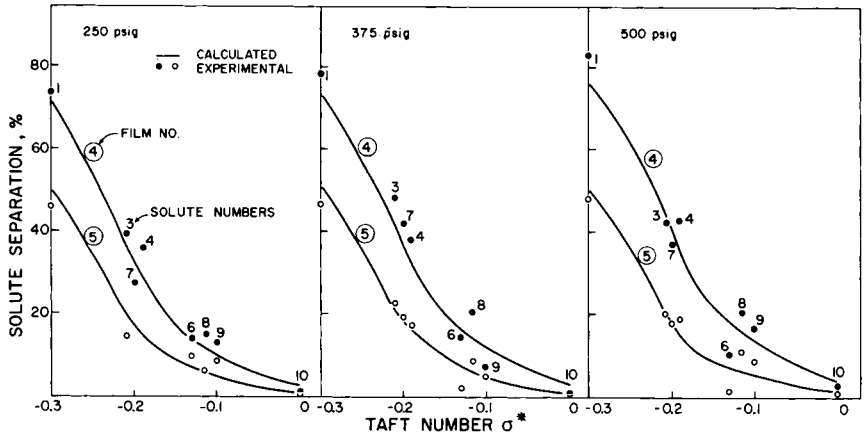

Fig. 5. Effect of Taft number on solute separation for alcohols for films 4 and 5: (——) predicted; (●) (○) experimental; film type, cellulose acetate (Batch 316); operating pressure, 250, 375, and 500 psig; feed flow rate, 400 cc/min; solute numbers, same as in Table I.

product rate was essentially the same as pure water permeation rate at the same operating pressure (obtained from data on membrane specifications given in Table II), solute separations for all the eight alcohols were back calculated for films 1, 2, and 3, using eqs. (1) and (5), at the operating pressures of 50, 250, 375, and 500 psig. In these calculations, the values of k used were the same as those used in the experiments (Table I). The results of the back calculations, illustrated in Figure 4, showed good agreement between experimental and calculated values for solute separation at operating pressures of 250, 375, and 500 psig. In the experimental system used, the magnitude of the exact operating pressure is subject to possible significant error at low pressures. In view of this possibility, the agreement obtained between the experimental and calculated values for solute separation at 50 psig must also be considered as reasonable. Consequently, the above results not only confirmed the validity of the transport equations used in the calculations, but also showed that the values of ρ^* and C^* used in the calculations were applicable for the pressure range of 50 to 500 psig.

In the second test, the performance of two new membrane samples, films 4 and 5, was considered. For purposes of calculations, *s*-butyl alcohol–water was arbitrarily chosen as the reference feed solution system. From the experimental $D_{AM}/K\delta$ values for *s*-butyl alcohol, the values of ln C^* for the above films were calculated to be -3.90 and -2.82, assuming $\rho^* = 15.5$ for both the films. Using the above ρ^* and C^* values, solute separations for the other seven alcohols were calculated as before, using eqs. 1 and 5 for the operating pressures of 250, 375, and 500 psig. The results were compared with the actual experimental data as shown in Figure 5. The agreement between the experimental and calculated data was again found to be excellent, confirming the validity of the transport equations and the prediction procedure discussed above.

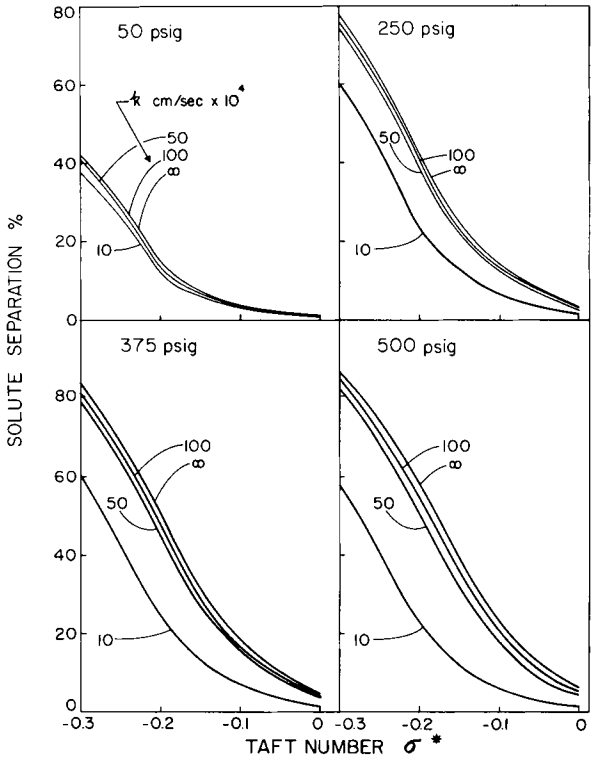

Fig. 6. Effect of mass transfer coefficient k on solute separation for alcohols for film 2 film type, cellulose acetate (Batch 316); operating pressure, 50, 250, 375, and 500 psig

Effect of Mass Transfer Coefficient k on Solute Separation. Figure 6 shows that σ^*-versus-solute separation correlation for a typical film (film 2) for k values of 10×10^{-4}, 50×10^{-4}, 100×10^{-4}, and ∞ cm/sec at the operating pressures of 50, 250, 375, and 500 psig. These correlations were generated using eqs. (1) and (5) with $\rho^* = 15.5$ and $\ln C^* = -3.70$, and assuming $PR \approx PWP$ at the given operating pressure. These correlations illustrate that with decrease in k, solute separation decreases, and the latter decrease is steep at values of k less than 50×10^{-4} cm/sec, especially at higher operating pressures. Consequently, it seems desirable to maintain a value of $k = 50\times10^{-4}$ cm/sec or higher in practical operations where higher solute separations are needed.

When solute separation data f are based on feed concentration, these data constitute a true reflection of the preferential sorption of water at the membrane–solution interface only when the boundary concentration is the same as the feed concentration. Such is the case only when $k = \infty$, under which condition $f = f_\infty$. Therefore, the data on f_∞ are of special interest. The value of f_∞ is given by eq. (6). When $D_{AM}/K\delta$, S, and d are constants, and PR is proportional to the effective pressure P_{eff}, eq. (6) reduces to

$$f_\infty = \frac{K_1 P_{eff}}{K_1 P_{eff} + 1} \tag{10}$$

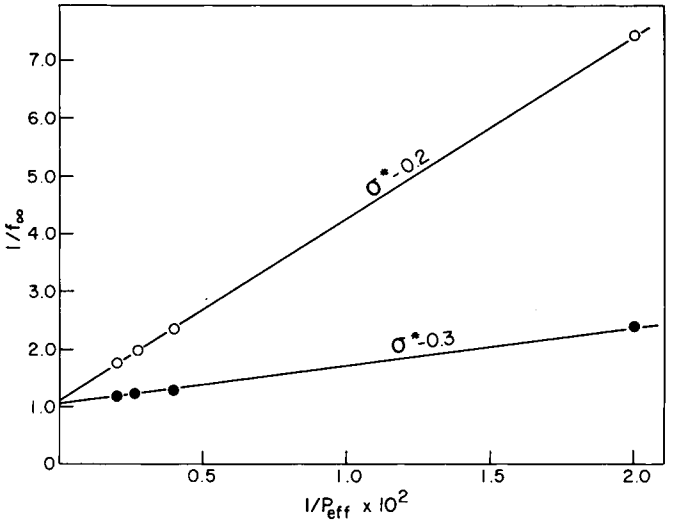

Fig. 7. Correlation of $1/f$ at $k = \infty$ vs. $1/P_{eff}$ for film 2: film type, cellulose acetate (Batch 316); σ^* of solutes, -0.2 and -0.3.

where K_1 is a constant, so that the plot of $1/f_\infty$ versus $1/P_{eff}$ is a straight line. Such plots are illustrated in Figure 7 for film 2 for σ^* values of -0.2 and -0.3, taking P_{eff} = operating pressure P, which is essentially the case at very low feed concentrations. It may be recalled that eq. (10) was formerly presented[6] on an empirical basis. The foregoing derivation gives eq. (10) a firm foundation in terms of reverse osmosis transport theory. Further, eq. (10) has the same form as the familiar Langmuir adsorption equation; as pointed out earlier,[6] this is not surprising on the basis that reverse osmosis separation is governed by preferential sorption at the membrane–solution interface.

The combined effect of operating pressure P and mass transfer coefficient k on solute separation is particularly interesting, as illustrated by the following analysis which is applicable to very dilute feed solutions only. Let v_s represent the permeation velocity (cm/sec) of product solution expressed by

$$v_s = \frac{PR}{3600\, S\, d}. \tag{11}$$

Equation (5) can then be written as

$$(D_{AM}/K\delta) = v_s \cdot \frac{1-f}{f}\,[1/\exp(v_s/k)] \tag{12}$$

or

$$\frac{1}{f} = 1 + \frac{(D_{AM}/K\delta)\exp(v_s/k)}{v_s} \tag{13}$$

$$\exp(v_s/k) = 1 + \frac{v_s}{k} + \frac{1}{2!}\left(\frac{v_s}{k}\right)^2 + \ldots. \tag{14}$$

When v_s/k is sufficiently small,

$$\exp(v_s/k) \approx 1 + \frac{v_s}{k} \tag{15}$$

and eq. (13) becomes

$$\frac{1}{f} = 1 + \frac{(D_{AM}/K\delta)(1 + v_s/k)}{v_s} \tag{16}$$

or

$$f = \frac{v_s}{v_s\left[1 + \frac{(D_{AM}/K\delta)}{k}\right] + (D_{AM}/K\delta)}. \tag{17}$$

When $D_{AM}/K\delta$ and k are constants and v_s is proportional to the effective pressure P_{eff}, eq. (17) becomes

$$f = \frac{K_2 P_{\text{eff}}}{K_3 P_{\text{eff}} + 1} \tag{18}$$

where K_2 and K_3 are constants. Equation (18) corresponds to the general form of the Langmuir adsorption equation. According to eq. (18), $1/f$ versus $1/P_{\text{eff}}$ is a straight line for constant values of $D_{AM}/K\delta$ and k; further, where eq. (18) is applicable, solute separation tends to increase with increase in operating pressure.

Equation (17) is subject to the restriction that v_s/k is small. When $v_s/k = 0.15$, the magnitude of the third term is less than 1% of the sum of the first two terms on the right side of eq. (14). Assuming 1% deviation is acceptable, eq. (18) can be expected to be valid when v_s/k is equal to or less than 0.15.

It is also interesting to consider eq. (13) subject only to the restriction that the values of $D_{AM}/K\delta$ and k are constant. With this restriction, let $\exp(v_s/k)/v_s$ be some function of v_s represented by the expression

$$F(v_s) = \frac{\exp(v_s/k)}{v_s}. \tag{19}$$

Differentiating eq. (19) with respect to v_s,

$$F'(v_s) = \frac{\exp(v_s/k)}{v_s^2}\left(\frac{v_s}{k} - 1\right) \tag{20}$$

which becomes zero when $v_s/k = 1$. Noting that $\exp(v_s/k)$ tends to increase with increase in v_s, eq. (14), eq. (20) predicts that the plot of $1/f$ versus v_s/k should exhibit a minimum, or the plot of f versus v_s/k should exhibit a maximum at $v_s/k = 1$. Since v_s should increase with increase in operating pressure, and $D_{AM}/K\delta$ and k may be practically independent of operating pressure at least with particular membrane–solution systems, eq. (20) predicts the possibility that solute separation may pass through a maximum with increase in operating pressure in some cases. No numerical

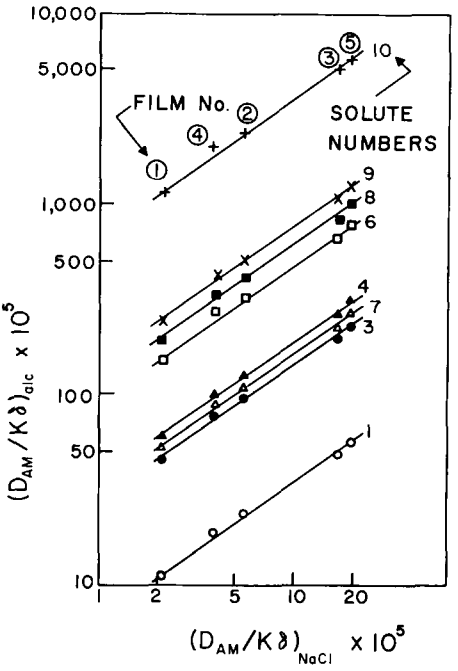

Fig. 8. Correlation of relative solute transport parameters for sodium chloride and alcohols: film type, cellulose acetate (Batch 316); operating pressure, 50 to 500 psig; solute numbers, same as in Table I.

data are presented in this paper to illustrate the above possibility, the existence of which, however, suggests the need for further theoretical and experimental work on the subject.

Correlation of Relative Solute Transport Parameters for Sodium Chloride and Alcohols. Figure 8 gives a plot of the relative values of the solute transport parameter for NaCl, $(D_{AM}/K\delta)_{NaCl}$, versus those for alcohols, $(D_{AM}/K\delta)_{alc}$, obtained with the five membrane samples (films 1, 2, 3, 4, and 5) and the eight alcohol–solutes studied. The data for $(D_{AM}/K\delta)_{NaCl}$ used were those obtained directly from experiments. The data for $(D_{AM}/K\delta)_{alc}$ used were those obtained from eq. (1) using the ρ^* and C^* values evaluated by the least-squares treatment of all the experimental data applicable for the operating pressure range of 50 to 500 psig. Figure 8 shows that log $(D_{AM}/K\delta)_{NaCl}$ versus log $(D_{AM}/K\delta)_{alc}$ is essentially a straight line whose slope is the same for all the eight alcohols studied. This result is an interesting and useful one since it links the values of $(D_{AM}/K\delta)_{alc}$ with those of $(D_{AM}/K\delta)_{NaCl}$ as follows. Equations (1) can be written as

$$\ln (D_{AM}/K\delta)_{alc} = \rho^*\sigma^* + \ln C^* \tag{21}$$

when

$$\sigma^* = 0, \ln C^* = \ln (D_{AM}/K\delta)_{alc(\sigma^*=0)}. \tag{22}$$

On the basis of Figure 8, let

$$\ln (D_{AM}/K\delta)_{\text{alc}(\sigma^*=0)} = a \ln (D_{AM}/K\delta)_{\text{NaCl}} + \ln b \tag{23}$$

where a and b are link constants, i.e., constants linking the relative $D_{AM}/K\delta$ values at $\sigma^* = 0$. Equation (21) becomes

$$\ln (D_{AM}/K\delta)_{\text{alc}} = a \ln (D_{AM}/K\delta)_{\text{NaCl}} + \rho^*\sigma^* + \ln b \tag{24}$$

or

$$(D_{AM}/K\delta)_{\text{alc}} = (D_{AM}/K\delta)^a_{\text{NaCl}} \times b \exp (\rho^*\sigma^*). \tag{25}$$

Thus, eq. (25) links the values of $(D_{AM}/K\delta)_{\text{alc}}$ with those of $(D_{AM}/K\delta)_{\text{NaCl}}$ through the link constants a and b and the parameters ρ^* and σ^*. The values of a and b can then be evaluated by the least-squares treatment of data on $(D_{AM}/K\delta)_{\text{NaCl}}$, $(D_{AM}/K\delta)_{\text{alc}}$, and the corresponding values of $\rho^*\sigma^*$. The values of a and b thus evaluated were found to be 0.699 and 23.0, respectively. Consequently, eq. (25) becomes

$$(D_{AM}/K\delta)_{\text{alc}} = (D_{AM}/K\delta)^{0.699}_{\text{NaCl}} \times 23.0 \exp (\rho^*\sigma^*). \tag{26}$$

The above equation enables one to calculate $(D_{AM}/K\delta)_{\text{alc}}$ in the σ^* range of 0 to -0.3 from the reverse osmosis data for the system NaCl–H_2O only, for the type of membranes used in this work.

It should be noted that the link constants a and b are explicitly defined in terms of eq. (23) applicable for the condition $\sigma^* = 0$. The final evaluation of a and b, however, involves the use of $(D_{AM}/K\delta)_{\text{alc}}$ data for all the eight alcohols in the σ^* range of 0 to -0.3. This procedure gives greater reliability for the numerical values of a and b.

Effect of Pore Structure on Membrane Surface on Alcohol Separation. Equation (13) can be written as

$$f = \frac{1}{1 + (D_{AM}/K\delta)_{\text{alc}} \dfrac{\exp (v_s/k)}{v_s}}. \tag{27}$$

Using eq. (26), eq. (27) becomes

$$f = \frac{1}{1 + (D_{AM}/K\delta)^{0.699}_{\text{NaCl}} \cdot 23.0 \dfrac{\exp (v_s/k)}{v_s} \exp (\rho^*\sigma^*)}. \tag{28}$$

Equation (28) can be written in the general form

$$f = \frac{1}{1 + \phi \exp (\rho^*\sigma^*)} \tag{29}$$

where

$$\phi = (D_{AM}/K\delta)^{0.699}_{\text{NaCl}} \cdot 23.0 \frac{\exp (v_s/k)}{v_s}. \tag{30}$$

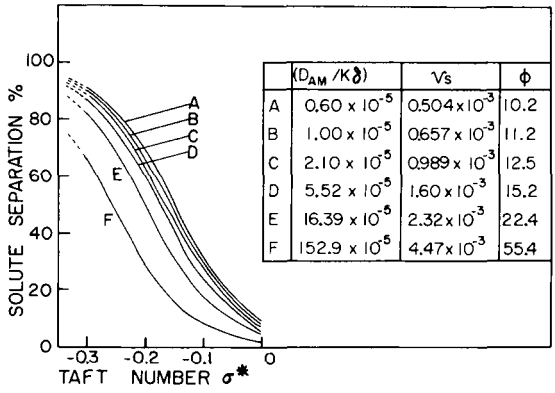

	$(D_{AM}/K\delta)$	v_s	ϕ
A	0.60×10^{-5}	0.504×10^{-3}	10.2
B	1.00×10^{-5}	0.657×10^{-3}	11.2
C	2.10×10^{-5}	0.989×10^{-3}	12.5
D	5.52×10^{-5}	1.60×10^{-3}	15.2
E	16.39×10^{-5}	2.32×10^{-3}	22.4
F	152.9×10^{-5}	4.47×10^{-3}	55.4

Fig. 9. Solute separation of alcohols at different values of ϕ: film type, cellulose acetate (Batch 316); operating pressure, 500 psig; mass transfer coefficient $k = \infty$.

Equations (29) and (30) are extremely useful and instructive with reference to reverse osmosis separation of solutes in very dilute aqueous solutions using porous cellulose acetate membranes.

Consider eqs. (29) and (30) for a given operating pressure at a given value of k. Under these conditions, the numerical values of $(D_{AM}/K\delta)_{\text{NaCl}}$ and v_s give a measure of the size and number of pores on the membrane surface. For a given membrane, the quantity ϕ is a constant. As the pore size decreases, the magnitude of ϕ decreases. Thus, the numerical value of ϕ is a function of the porous structure of the membrane surface. Equation (29) predicts solute separation for any alcohol obtainable with any membrane whose surface pore structure is defined by eq. (30). Thus, eq. (29) expresses the effect of pore structure on membrane surface on alcohol separation. One can assign different numerical values of ϕ and calculate f using eq. (29). This is illustrated in Figure 9 for the case $k = \infty$ and operating pressure = 500 psig. Figure 9 shows that with a sufficiently small average pore size on membrane surface, solute separation tends towards 100% for all alcohols. For a given value of ϕ (i.e., given values of $(D_{AM}/K\delta)$, v_s, and k), eq. (29) expresses the effect of solute polarity on reverse osmosis separation.

Equation (29) also indicates that the value of ρ^* would tend to infinity as the value of σ^* tends to that of water. The experimental data on log $(D_{AM}/K\delta)_{\text{alc}}$ versus σ^* presented earlier[5] tend to support this conclusion, which means that log $(D_{AM}/K\delta)_{\text{alc}}$ is a continuous function of σ^*, and the assumption of constant ρ^* is a practical approximation valid only for small ranges of σ^*. The form of eq. (29) probably has general validity for reverse osmosis separation of water at membrane–solution interfaces. This possibility opens a new area of investigations in reverse osmosis transport.

Mixed Solute Systems

Effect of Mixed Solutes on Solute Separation. The effect of mixed solutes on membrane performance was ascertained by reverse osmosis ex-

periments using several membrane samples of different surface porosities. The following mixed solute systems were studied: (1) *t*-butyl alcohol + *s*-butyl alcohol, (2) *t*-butyl alcohol + isopropyl alcohol. (3) *t*-butyl alcohol + isobutyl alcohol, (4) *t*-butyl alcohol + *n*-propyl alcohol, (5) *t*-butyl alcohol + *s*-butyl alcohol + *n*-butyl alcohol + isobutyl alcohol + isopropyl alcohol, (6) *s*-butyl alcohol + isopropyl alcohol, and (7) isobutyl alcohol + isopropyl alcohol.

The solute concentration used was 0.002 g mole/l. with respect to each alcohol. Each system was studied at three operating pressures, namely, 50, 250, and 500 psig. At each operating pressure, the product rates obtained were essentially the same for all the mixed solute systems studied. With respect to solute separation, the data obtained for the separations of *t*-butyl alcohol, *s*-butyl alcohol, isopropyl alcohol, and isobutyl alcohol in mixed solute systems were compared with the corresponding data obtained in single solute systems. The results, given in Figure 10, showed that within the limits of experimental error, the separations for each alcohol in the single and mixed solute systems were essentially identical indicating that the alcohol-solutes behave independently in reverse osmosis. This means that alcohol separations obtainable for mixed solute systems are the same as those obtained or predicted for single solute systems. This result is of practical significance in fruit juice concentration by reverse osmosis.

Separation of Alcohol Present in Aqueous Sucrose Feed Solutions. The separation of alcohol present in low concentrations in aqueous solutions of sucrose present in high concentrations is of practical interest from the point of view of retention of flavor components during the reverse osmosis concentration of fruit juices. With appropriate choice for the surface porosities, membranes can be found to give essentially complete solute separation with respect to sucrose under the operating conditions used. Even with such membranes, solute separation for alcohol will be much less with an aqueous sucrose feed solution than with plain aqueous feed solution without any sucrose.

Two factors are responsible for the above decrease in alcohol separation. With an aqueous sucrose feed solution, the effective pressure for fluid flow (water transport) through the membrane is reduced because of the high osmotic pressure of sucrose solutions, and the mass transfer coefficient for the alcohol (k_{alc}) on the high-pressure side of the membrane is also reduced because of the high viscosity of sucrose solutions. Since these two factors are amenable to theoretical analysis, it should be possible to predict alcohol separation as a function of sucrose concentration in feed under given conditions of operating pressure and feed flow rate with a properly specified membrane. This possibility is illustrated below by a set of experiments with three membrane samples (films 1, 2, and 3) for the separation of *t*-butyl alcohol in aqueous sucrose feed solutions.

The operating pressure employed in these studies was 350 psig, and the feed flow rate was kept constant ($\sim$400 cc/min) in all the experiments. The concentration of *t*-butyl alcohol in the feed solution was 2.0×10^{-3}

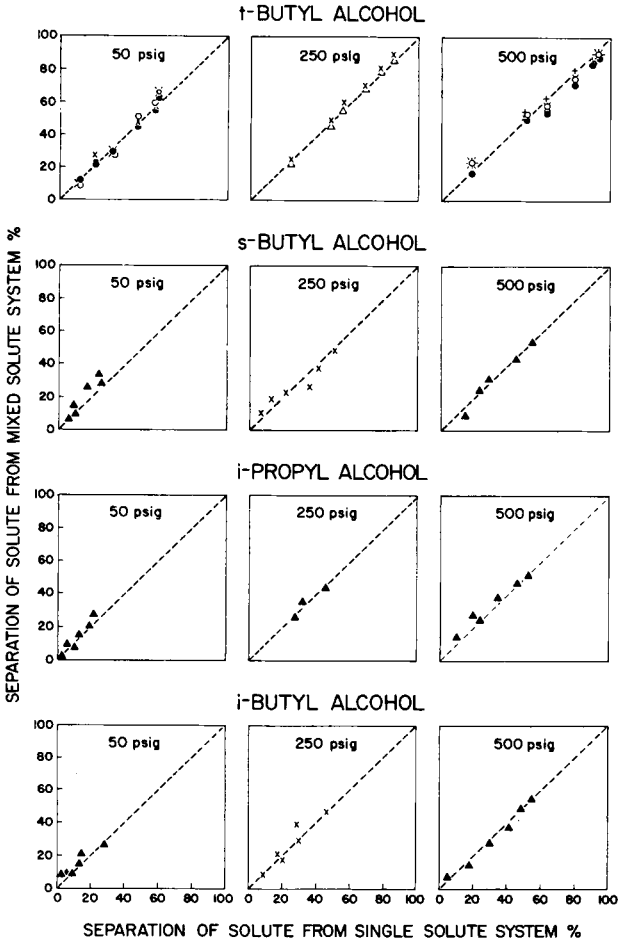

Fig. 10. Comparison of the solute separation in single solute system with the corresponding data in mixed solute system: solutes written in the figure mixed with (▲) *t*-butyl alcohol; (○) *s*-butyl alcohol; (×) isopropyl alcohol; (●) isobutyl alcohol; (+) *n*-propyl alcohol; (△) *s*-butyl alcohol, isopropyl alcohol, *n*-butyl alcohol, plus isobutyl alcohol; film type, cellulose acetate (Batch 316); feed concentration 0.002 g-mole/l. for each solute; feed flow rate, 400 cc/min.

molal (~150 ppm) in each experiment. The sucrose concentration in the feed solution ranged from 0 to 0.5853 molal (0 to 16.69 wt-%). At the operating pressure and feed flow rate used, the separations of *t*-butyl alcohol in aqueous solution without any sucrose were 80%, 70%, and 58% with films 1, 2, and 3, respectively. With 0.5853 molal aqueous sucrose feed solution, the corresponding alcohol separations were 41%, 24%, and 10%.

From the PWP, PR, and sucrose separation data, the values of A, $(D_{AM}/K\delta)_{\text{sucrose}}$, and mass transfer coefficient for sucrose (k_{sucrose}) on the high-pressure side of the membrane were calculated by the Kimura-Sourirajan analysis.[6] Generally, for the system sucrose–water, the value of $(D_{AM}/$-

TABLE IV
Data for Sucrose–*t*-Butyl Alcohol–Water Solution System
Specifications of Membranes Used[a]

Sucrose concn. in feed		Kinematic viscosity × 10^2,	$k_{sucrose}$ × 10^4,
Molality	wt-%	cm/sec	cm/sec
0.1148	3.78	0.972	8.2
0.2440	7.71	1.070	7.1
0.3747	11.37	1.183	6.6
0.4990	14.59	1.302	5.0
0.5853	16.69	1.396	3.2

$X_{A2(sucrose)}$ × 10^3	$D_{sucrose}$ × 10^5, cm²/sec	D_{alc} × 10^5, cm²/sec	k_{alc} × 10^4, cm/sec
	Data for film 1		
3.980	0.497	0.862	11.8
7.421	0.482	0.727	9.4
10.41	0.473	0.627	7.9
12.89	0.466	0.552	5.6
14.51	0.452	0.507	3.5
	Data for film 2		
5.507	0.490	0.796	11.3
9.351	0.476	0.662	8.9
11.71	0.469	0.586	7.6
13.73	0.464	0.528	5.5
14.94	0.462	0.497	3.4
	Data for film 3		
6.144	0.487	0.773	11.1
9.982	0.474	0.641	8.7
12.28	0.468	0.569	7.5
14.05	0.464	0.519	5.4
15.16	0.461	0.490	3.3

[a] Operating pressure: 350 psig.
Film Specifications:

Films	1	2	3
A(g-mole H_2O/cm² sec atm) × 10^6	1.61	2.61	3.78
Av. $(D_{AM}/K\delta)_{sucrose}$ (cm/sec) × 10^5	0.046	0.035	0.106

Concn. of *t*-BuOH in feed: 2.0 × 10^{-3} molal.

$K\delta)_{sucrose}$ tends to decrease with increase in feed concentration; this tendency, however, is negligible at low operating pressures, particularly when the magnitude of the above parameter is itself very small as is the case in the above experiments.[10] Further, for practical purposes, the mass transfer coefficient on the high-pressure side of the membrane may be considered to be independent of the porous structure of the membrane. Consequently, for purposes of analysis, average values of $(D_{AM}/K\delta)_{sucrose}$ and $k_{sucrose}$ can be used. These values are given in Table IV.

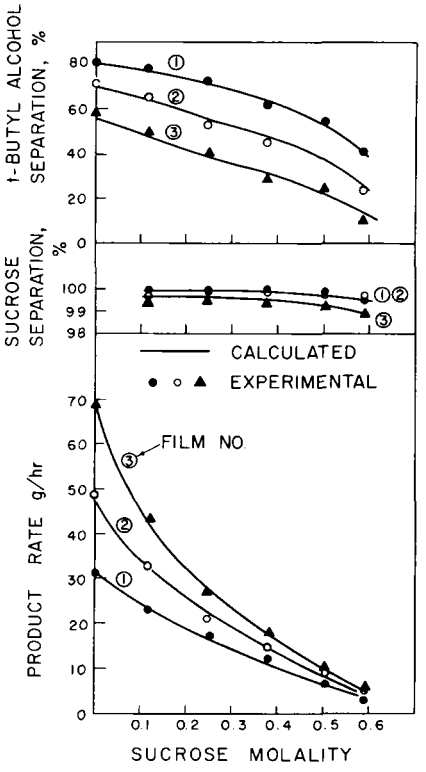

Fig. 11. Effect of sucrose concentration on the separations of sucrose and *t*-butyl alcohol and on product rate for films 1, 2, and 3: (——) predicted; (●) (○) (▲) experimental; film type, cellulose acetate (Batch 316); operating pressure, 350 psig; feed concentration of *t*-butyl alcohol, 0.002 molality; feed flow rate, 400 cc/min; membrane area, 13.2 cm².

The values of $(D_{AM}/K\delta)_{\text{sucrose}}$ given in Table IV are applicable for all the sucrose concentrations used in the feed solution, and the values of k_{sucrose} given are applicable for all the three films studied. This was confirmed by the back calculation of product rates and sucrose separations using the the values of A, $(D_{AM}/K\delta)_{\text{sucrose}}$, and k_{sucrose} given in Table IV for films 1, 2 and 3. The results obtained (solid lines) are given in Figure 11 along with the experimental data. There was excellent agreement between the calculated and experimental data.

For predicting alcohol separations in aqueous sucrose solutions, the first step is to calculate the applicable mass transfer coefficients for the alcohol (k_{alc}) under the experimental conditions. This is done by using eq. (4) with sucrose–water as the reference solution system. Thus, eq. (4) can be rewritten as

$$k_{\text{alc}} = k_{\text{sucrose}} \left[\frac{D_{\text{alc}}}{D_{\text{sucrose}}} \right]^{2/3}$$

where D_{alc} is the diffusivity of alcohol in the aqueous sucrose solution and $D_{sucrose}$ is the diffusivity of sucrose in water. For calculating the values of D_{alc} and $D_{sucrose}$, the concentration of sucrose in the boundary solution (i.e. the mole fraction of sucrose in the concentrated boundary solution, $X_{A2(sucrose)}$) under the actual experimental conditions employed was used. The values of $X_{A2(sucrose)}$ were determined by the Kimura-Sourirajan analysis of experimental data for each film.[6] The values of $D_{sucrose}$ at $X_{A2(sucrose)}$ were obtained from the literature,[6] and the corresponding values of D_{alc} were calculated from the equation of Wilke and Chang,[9] using the viscosity (obtained from the literature)[6] of aqueous sucrose solution corresponding to $X_{A2(sucrose)}$. The values of $X_{A2(sucrose)}$, $D_{sucrose}$, D_{alc}, and k_{alc} obtained in the experiments reported here are given in Table IV.

The next step is to use the value of k_{alc} calculated above in eq. (5) or its equivalent eq. (13) to predict solute separation for alcohol. For using any of the above equations, data on $D_{AM}/K\delta$ for the alcohol and PR are needed. The data on $D_{AM}/K\delta$ for *t*-butyl alcohol for each of the above films were obtained from eq. (1) using the known values of ρ^* (= 15.5), σ^* (= −0.3), and C^* (= −4.46, −3.70, and −2.99 for films 1, 2, and 3, respectively). The PR data used were the same as those obtained in the reverse osmosis experiments with the *t*-butyl alcohol–sucrose–water system. The values of alcohol separation obtained from such calculations are given in Figure 10 (solid lines) along with experimental values. The agreement between calculated and experimental values was excellent. These results illustrate not only the precise reasons for decrease in alcohol separations in aqueous sucrose feed solutions, but also confirm the validity of the procedure used above for predicting such separations.

Conclusions

The data presented in this paper offer further experimental confirmation of the validity and usefulness of the Taft number criterion for the relative separation of alcohols in aqueous solutions. The results also illustrate the applicability of Equation 1 in reverse osmosis transport for predicting membrane performance in single and mixed solute systems.

The authors are grateful to J. M. Dickson, Lucien Pageau, and A. G. Baxter for their assistance in the progress of these investigations. Issued as N.R.C. No. 13752.

References

1. R. E. Kesting and J. Eberlin, *J. Appl. Polym. Sci.*, **10**, 961 (1966).
2. W. A. Duvel, Jr., T. Helfgott, and E. J. Genetelli, paper presented before the ACS Division of Water, Air and Waste Chemistry, Chicago Meeting, September 1970.
3. T. Matsuura and S. Sourirajan, *J. Appl. Polym. Sci.*, **15**, 2905 (1971).
4. W. A. Duvel, Jr., T. Helfgott, and E. J. Genetelli, *A.I.Ch.E. Symp. Ser.*, **68**, (124), 250 (1972).
5. T. Matsuura and S. Sourirajan, *J. Appl. Polym. Sci.*, **17**, 1043 (1973).
6. S. Sourirajan, *Reverse Osmosis*, Academic Press, New York, 1970, Chap. 3.

7. B. Kunst and S. Sourirajan, *J. Appl. Polym. Sci.*, **14**, 2559 (1970).
8. R. W. Taft, Jr., in *Steric Effects in Organic Chemistry*, M. S. Newman, Ed., Wiley, New York, 1956, p. 619.
9. C. R. Wilke and P. Chang, A.I.Ch.E.J., **1**, 264 (1955).
10. T. Matsuura, A. G. Baxter, and S. Sourirajan, *Acta Alim.* **2**(2), 109 (1973).

Received June 15, 1973